Multi-Robot System Maintained with Distributed Renewable Energy Sources

Jaehyun Kim and Chanwoo Moon
School of Electrical Engineering, Kookmin University, Seoul, Republic of Korea
Email: goss818@gmail.com, mcwnt@kookmin.ac.kr

***Abstract*—It is difficult for robots working in a large outdoor area to receive energy from a stable commercial power source. In this case, renewable energy sources could be used to supply energy to the robot. In this paper, we present a multi-robot autonomy system that obtains energy from distributed small-scale renewable energy sources with limited storage capacity. A model based on an energy production–consumption equilibrium equation was developed to judge whether the robot could survive with the energy obtained from the allocated energy sources, and a heuristic method was proposed to improve robot utility by allocating energy nodes to each robot based on a k-means algorithm and reallocating energy sources in the border region. Finally, a small-scale renewable energy source that transfers energy by means of Wireless Power Transfer (WPT) was constructed, and a charge experiment was conducted to verify the feasibility of the proposed robot energy autonomy system.**

***Index Terms*—Multi-robot autonomy, Small-scale renewable energy, Production–consumption model, Wireless power transfer, k-means algorithm**

I. Introduction

With the development of autonomous driving technology and artificial intelligence, diverse applications of mobile robots have emerged in multiple domains, such as agriculture, delivery, search, and exploration. Research on the use of multi-mobile-robot systems to perform tasks such as logistics and transportation of heavy objects is being conducted actively. A multi-robot system can more efficiently execute complex tasks that are difficult for a single robot. With an increase in the number of robots used in such systems, there has been a growing interest in robot autonomy systems, namely robot systems that are operated with minimal intervention from a human operator [1,2]. However, the issue of energy supply to the robots must be solved before robot autonomy can be achieved.

Home robots typically recharge automatically, and the robot locates the recharge station [3,4]. Typically, commercial power sources are used to charge robots. However, various energy sources for mobile robots have been considered for scenarios in which a stable commercial power supply may not be available. One typical example is photovoltaic cells. Although they have been widely adopted, it is difficult to use them in the absence of sunlight or with payload limitations. In scenarios where energy cannot be supplied from a commercial power source, an alternative method is to receive energy from external renewable energy generators, such as wind and solar power generators. Khonji proposed a drone charging system that used wireless power transmitted from a solar generator that was sufficiently large to charge a robot directly without storing energy, but they did not consider whether the robot could survive on the acquired energy [5].

In multi-robot systems, the charging problem is exacerbated because of several peculiar challenges such as recharge priority and charger allocation. Assuming a limited number of charging stations, one study used algorithms to allocate charging stations depending on robot charging status and priorities [6]. In another study, robots that charge autonomously and perform surveillance operations in national parks were used [7].

In the case of robots working in large areas such as forests or fields, it is difficult to supply power from commercial power sources. As alternatives, distributed renewable energy generators can be used as energy sources for such robots. Three cases can be considered based on generator capacity:

i) The power capacity of the generator is large. In this case, there is no difference compared to receiving energy from a commercial power source.

ii) The power capacity of the generator is small but the capacity to store the generated energy is adequately large to charge a robot in one charging session.

iii) The power and storage capacities are small.

In the second and third cases, a robot must obtain energy from multiple generators to survive. However, the methods by which the robot obtains energy from the generator differ. In the second case, it would be reasonable for the robots comprising a multi-robot system to charge themselves by taking turns to visit the generator.

In a previous study [8], we proposed a single-robot system that survived by acquiring energy from a distributed, small-scale renewable energy source with limited storage capacity (the third case listed above), and we derived the survival conditions of the robot by using the dynamic equation of acquired energy. In this study, we extend the previous research to a multi-robot system

Manuscript received November 23, 2021; revised January 17, 2022.
Corresponding author: Chanwoo Moon

doi: 10.18178/ijmerr.11.6.389-398

powered using a distributed small-scale renewable energy source, which is similar to the behavior of a biome. The survival conditions of the robot system are re-derived based on the energy production–consumption equilibrium condition instead of the previously presented dynamic equation. A heuristic method for allocating energy nodes to each robot based on a modified k-means method is proposed. A small-scale thermoelectric energy module (TEM) is constructed, and charging experiments conducted to verify the feasibility of the proposed energy autonomy system are described.

The remainder of this paper is organized as follows. Section II presents the problem statement and subsequent energy production–consumption model. Section III presents the numerical evaluations of the proposed system, and in Section IV, the experimental results are given. A summary of the paper is provided in Section V.

II. Multi-robot Energy Autonomy Model

A. Problem Statement

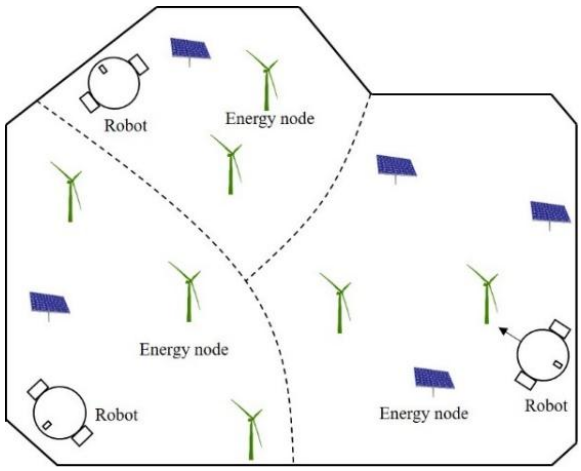

Figure 1. Multi-robot workspace

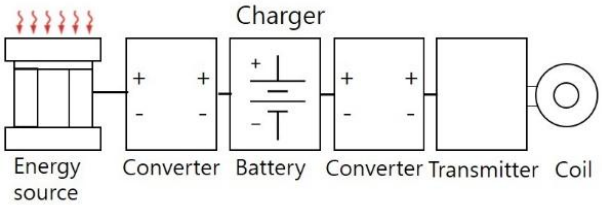

Figure 2. Typical energy node structure

The robot energy autonomy problem considered herein consists of multiple robots and renewable energy production nodes. As depicted in Fig. 1, small-scale renewable energy production nodes are distributed over a wide area. When the energy level of a robot is close to exhaustion, the robot visits these energy nodes to recharge. When a robot visits an energy node, it can take an arbitrary path. However, it follows a Hamiltonian path to minimize the energy consumption required for movement [9]. Because the power generation capacity of the energy node is small, to ensure that it can operate, the robot must obtain energy from one or more energy nodes. Each energy node stores generated electrical energy in a battery with limited capacity and transmits this energy to the robot during the charging process. In conventional automatic charging methods, mechanical contact is used [3]. However, electrical contact is often incomplete in outdoor environments, where the charging terminal can be contaminated [10]. Therefore, we use wireless power transfer (WPT) to solve this problem associated with conventional energy transfer. Several studies have considered the use of WPT for charging mobile robots. For example, in [10,11], an automatic mobile robot charging system based on image information was proposed. In [12], a WPT-based charging system for rotary-wing drones was proposed. Fig. 2 illustrates the structure of a typical energy node, which includes an energy source, a power converter, an energy storage (ES) system, and a transmitter and coil for power transmission. [8]

B. Charge Cycle Model

In this section, we construct a model that represents energy production at the energy node and energy consumption of the robots.

1) Energy generation model [8]

The energy to be generated and transferred is approximated using a linear model, where the amount of energy produced is proportional to time and saturation level of the available storage capacity; moreover, the amount of energy delivered using WPT is proportional to the delivery time as follows:

$$\epsilon_i = \mathrm{sat}_{E_i}\left(g_i \cdot t_g + \epsilon_{i0}\right), \quad (1)$$

$$e_{iT} = \mu \cdot t_T, \quad (2)$$

And

$$e_{iR} = \eta \cdot \mu \cdot t_T, \quad (3)$$

where ϵ_i is the stored energy (initially ϵ_{i0}); g_i is the energy generation rate; E_i is the ES capacity; e_{iT} and e_{iR} are the energies transmitted and received, respectively, from energy node i on the robot side; t_g is the duration of energy generation; μ is the WPT coil energy transfer rate; η is the energy transfer efficiency; t_T is the transmission duration; and the saturation function with L as the limit is defined as follows.

$$\mathrm{sat}_L(x) = x, if\ x < L$$
$$= L, if\ x \geq L$$

Because the energy transfer efficiency η is less than 1, only a fraction of the energy produced is used by the robot. Energy transfer efficiency is the product of WPT efficiency η_1, robot battery energy efficiency η_2, and power converter efficiency η_3, i.e., $\eta = \eta_1 \eta_2 \eta_3$. WPT efficiency depends on how well the transmitting and receiving coils are aligned, and we determined experimentally that $\eta_1 < 0.8$ for induction-type WPT systems. Battery energy efficiency is the ratio of usable energy to the energy received, and $\eta_2 \approx 0.8$ for Li-ion batteries, but it can be lower for other types of batteries [13]. Power converter efficiency η_3 was estimated to be 80% to 90%.

2) Energy consumption model

The robot power drains during robot movement and when the robot is stationary are P_{move} and P_{rest}, respectively. P_{rest}

is the power consumed by the controller board for robot control. P_{move} is the robot power consumption during driving, i.e., by the motors and sensors used for navigation and the controller [14].

The work phase and charge phase constitute one operation cycle. Several robots have a sleep (or idle) function. The power consumption in the sleep state P_{sleep} is the minimum about of power required to maintain the system, and it is significantly less than the power consumed during normal robot operation. The robot can enter a sleep state if the energy production at a node is insufficient. Fig. 3 illustrates a typical robot system operation–charge cycle. Table I presents the symbols used in the charge model.

C. Survival Condition of a Robot under Equilibrium Conditions

In a previous study [8], we derived a survival condition for a single-robot system by using a discrete dynamic equation of robot energy. If the energy consumed by the robot and that generated by the energy node are balanced, the robot can survive. Instead of the dynamic equation, we re-derive the robot survival condition by using the energy balance condition and obtain a simpler formula to achieve the same result as that in the previous study. The time t_{total} required for one production–consumption cycle is computed as follows:

$$t_{total} = t_{work} + t_{sleep} + t_{recharge} \quad (4)$$

where t_{work} is the robot working time, t_{sleep} is the time for which the robot is in a sleep state, and $t_{recharge}$ is the time required for energy acquisition. Moreover, $t_{recharge}$ is the sum of the time required for the robot to move between energy nodes t_{trip} and the time required for the robot to charge at the energy nodes t_{node}, as follows:

$$t_{recharge} = t_{trip} + t_{node}. \quad (5)$$

t_{trip} is a constant when the path is predetermined and given as $\frac{d}{g}$ on a flat terrain. Suppose N energy nodes are uniformly distributed over a square area of side length D (m) and are visited by following a Hamiltonian cycle. Then, the distance to be traveled d can be approximated as follows [9]:

$$0.625D < \lim_{N\to\infty} N^{-\frac{1}{2}} \cdot d < 0.922D \quad (6)$$

The energy generated during one cycle can be computed using (7), where Ψ_{E_S} is a function of time and denotes the total energy produced and stored. E_S is the total ES capacity of the nodes.

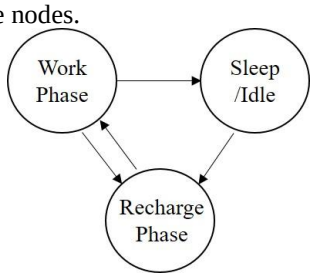

Figure 3. Typical robot operation–charge cycle.

TABLE I. SYMBOLS USED IN THE CHARGE MODEL.

Symbol	Explanation
ε_{total}	Total energy generation rate of all nodes (W)
μ	Energy transfer rate of WPT coil (W)
η	Energy transfer efficiency
x_i	Position of i_{th} Node
P_{rest}	Robot power consumption when stationary (W)
P_{move}	Robot power consumption during driving (W)
P_{work}	Average robot power consumption during operation (W)
P_{sleep}	Robot power consumption for sleeping (W)
t_{trip}	Total trip time for visiting energy nodes
d	Total trip distance for visiting energy nodes (m)
r	Robot speed (m/s)
$R(t)$	Robot energy at time t
E_S	Total energy storage capacity of nodes (J)
N	Number of energy nodes
K	Number of robots

$$\Psi_{E_S}(t_{total}) = \Psi_{E_S}(t_{work} + t_{sleep} + t_{recharge}) \quad (7)$$

In contrast to the individual energy generation function given in (1), Ψ_{E_S} is not a saturation function, but it can be approximated as a saturation function. Fig. 4 illustrates a typical Ψ_{E_S} function. Moreover, assuming that the storage capacity of each node is proportional to the node energy generation rate, the energy saturation of the entire node is expressed in terms of the saturation function, as follows:

$$\Psi_{E_S}(t) = \min(\varepsilon_{total}t, E_S). \quad (8)$$

The time t_1 for saturation is given as follows:

$$t_1 = \frac{E_S}{\varepsilon_{total}}. \quad (9)$$

The energy consumed during one cycle W_{total} is as follows:

$$W_{total} = P_{work}t_{work} + P_{sleep}t_{sleep} + P_{move}t_{trip} + P_{rest}t_{node}. \quad (10)$$

For a robot without sleep ability, $t_{sleep} = 0$, and the equilibrium condition is expressed as follows:

$$P_{work}t_{work} + P_{move} \cdot t_{trip} + P_{rest}t_{node} = \eta\Psi_{E_S}(t_{work} + t_{recharge}). \quad (11)$$

If WPT is used, the time required for the robot to charge is proportional to the energy delivered. Therefore, t_{node} is given as follows:

$$t_{node} = \Psi_{E_S}(t_{work} + t_{recharge})/\mu \quad (12)$$

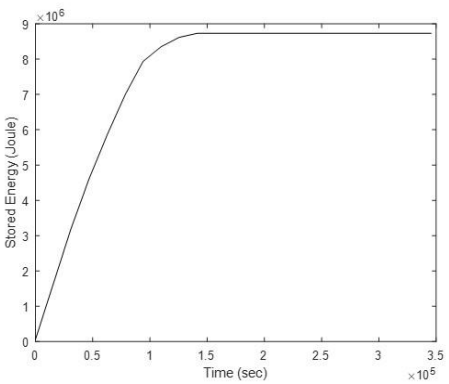

Figure 4. Produced and stored energy $\Psi(\cdot)$.

In equilibrium, let the time the robot spends working be t_{work_eq} and the time it spends charging in the energy node be t_{node_eq}. It can be divided into two cases: equilibrium is reached after the energy storage system is saturated, and equilibrium occurs before the energy storage system is saturated.

Case 1: If equilibrium is reached after the energy storage system is saturated, that is, $\Psi_{E_S}(t) = E_S$ and $t_{work} + t_{recharge} \geq t_1$, then from (11), t_{work_eq} and t_{node_eq} can be computed using (13) and (14), respectively:

$$t_{work\_eq} = ((\eta - \frac{P_{rest}}{\mu}) E_S - P_{move} \cdot t_{trip})/P_{work} \quad (13)$$

$$t_{node\_eq} = E_S/\mu \quad (14)$$

A feasible solution exists if $t_{work\_eq} > 0$ *and* $t_{work\_eq} > \frac{E_S}{\varepsilon_{total}} - t_{trip} - \frac{E_S}{\mu}$.

Case 2: If equilibrium is reached before saturation, that is, $\Psi_{E_S}(t) = \varepsilon_{total} \cdot (t_{work} + t_{recharge})$ and $t_{work} + t_{recharge} < t_1$, then from (11), t_{work_eq} and t_{node_eq} can be computed using (15) and (16), respectively:

$$t_{work\_eq} = (\frac{(P_{work} - P_{move})(\frac{\mu}{\varepsilon} - 1)}{P_{work}(\frac{\mu}{\varepsilon_{total}} - 1) + P_{rest} - \mu\eta} - 1) t_{trip} \quad (15)$$

$$t_{node\_eq} = \frac{(P_{work} - P_{move})}{P_{work}(\frac{\mu}{\varepsilon_{total}} - 1) + P_{rest} - \mu\eta} \cdot t_{trip}. \quad (16)$$

A feasible solution exists if $t_{work\_eq}, t_{node\_eq} > 0$ and $t_{work\_eq} + t_{node\_eq} < \frac{M}{\varepsilon_{total}} - t_{trip}$.

Fig. 5 shows a graph of energy production and consumption versus time. Equilibrium condition 1 can be determined using (15) and (16), equilibrium condition 2 can be determined using (13) and (14). The intersection that occurs in the area to the left of the dashed line is an infeasible solution because the robot's working time is a negative number in this case. Under the condition that the robot survives, because the energy consumption slope is gentler than the energy production slope, only equilibrium condition 2 or both equilibrium conditions 1 and 2 can exist. Given that the ratio of the time required to work to the energy acquisition time is high, the robot operates in Equilibrium condition 2, not Equilibrium condition 1.

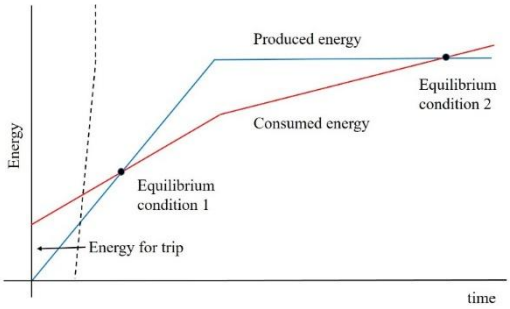

Figure 5. Energy produced and consumed.

A robot with a sleep function can survive if the equilibrium condition is satisfied in the sleep state. Similarly, according to the above procedure, survival conditions can be determined using (17) for a robot with a sleep function.

$$t_{sleep\_eq} = ((\eta - \frac{P_{rest}}{\mu}) E_S - P_{move} \cdot t_{trip})/P_{sleep} \quad (17)$$

t_{node_eq} is the same as in (14), and a feasible solution exists if $t_{sleep\_eq} > 0$ and $t_{sleep\_eq} > \frac{E_S}{\varepsilon_{total}} - t_{trip} - \frac{E_S}{\mu}$.

D. Recharge Strategy

A robot with no sleep function must visit an energy node when its energy level reaches zero. By contrast, a robot with a sleep function that runs out of energy during operation can enter a sleep state until it reaches the equilibrium point. In either case, a recharge strategy involves obtaining a high utilization rate *u* in (18), i.e., the proportion of time spent working relative to the total time.

$$u = \frac{t_{work}}{t_{work} + t_{sleep} + t_{recharge}} \quad (18)$$

Therefore, the charging strategy can be summarized as follows:

- Robot without sleep ability

Work phase → recharge mode
  if $R(t) \leq R_0$
Recharge mode → work
After charging is complete

where *t* is the current time, and R_o is the bottom energy, i.e., the minimum energy to ensure that the robot's energy is not entirely exhausted when it moves to acquire energy, regardless of the order in which the nodes are visited:

$$R(t) = R_{usable}(t) + R_o \quad (19)$$

$R_{usable}(t)$ is the total usable energy during the work phase. We formulate the recharge strategy of a robot with a sleep function based on the equilibrium state of the robot that works for a certain duration and sleeps for the rest of the time. Let T_{ws} be the time at which the robot departs toward the nodes to charge at equilibrium.

$$T_{ws} = t_{work\_eq} + t_{sleep\_eq} \quad (20)$$

Then, for $\lambda, 0 \leq \lambda \leq 1$:

$$t_{work\_eq} = \lambda T_{ws} \quad (21)$$

$$t_{sleep\_eq} = (1 - \lambda) T_{ws} \quad (22)$$

The average power consumption P_{ws} in the work area is given as follows:

$$P_{ws} = \lambda P_{work} + (1 - \lambda) P_{sleep} \quad (23)$$

From the equilibrium condition, again

$$\lambda = \frac{((\eta - P_{rest}/\mu) E_S - P_{move} \cdot t_{trip})/(E_S/\boldsymbol{\varepsilon_{total}} - t_{trip} - E_S/\mu) - P_{sleep}}{P_{work} - P_{sleep}} \quad (24)$$

$$T_{ws} = ((\eta - \frac{P_{rest}}{\mu}) E_S - P_{move} \cdot t_{trip})/P_{ws} \quad (25)$$

Finally, the charge strategy for a robot with sleep ability is as follows:

- Robot with sleep ability

Work phase → sleep

$t + (R(t) - R_o)/P_{sleep} \leq T_{ws}$

Work phase → recharge phase

if $R(t) \leq R_0$

Sleep → recharge phase

$t \geq T_{ws}$ or $R(t) \leq R_0$

Recharge phase → work

After visiting all of the nodes

E. Heuristic Node Allocation Method

When allocating energy nodes to robots, it is desirable to allocate them such that the performance of the robot group is improved. However, the number of methods available for allocating all energy nodes to robots is K^N. As the number of robots and nodes increases, this number becomes intractable. It is reasonable to allocate nearby energy nodes to one robot to shorten its movement path.

We propose a heuristic node allocation method that can improve robot performance. In the first step, clusters of adjacent nodes are identified using the k-means algorithm [15]. The nodes on the peripheries of the clusters are then adjusted based on the cluster with which they should be associated to increase the object function J (a higher value is desirable). The complete allocation method is as follows.

- Pre-allocation: k-means algorithm

  Initialization step

  While initial centroids are random data points in the classic k-means algorithm, the initial centroids $m_j^{(1)}$ of each robot $j = 1 \ldots K$ are selected manually based on prior knowledge.

  p_{th} Loop

  ① Consider the j_{th} cluster c_j $j = 1 \ldots K$:

$$c_j^{(p)} = \left\{ x_q : \left\| x_q - m_j^{(p)} \right\|^2 \leq \left\| x_q - m_i^{(p)} \right\|^2 \right\},$$

$$i = 1 \ldots K, i \neq j \quad (26)$$

$$m_j^{(p+1)} = \frac{1}{\left| c_j^{(p)} \right|} \sum_{x_q \in c_j^{(p)}} x_q \quad (27)$$

  ② Repeat until there is no change in clusters.

- Heuristic allocation adjustment method

  For an object function J and design parameter α, we have the following:

  q_{th} Loop

  ① Draw covariance error ellipse [16] for each cluster $c_j^{(q)}$ with confidence α, as depicted in Fig. 6.

  ② Select nodes belonging to multiple ellipses simultaneously, and change the cluster to which a node belongs, as follows:

  $n_j^{(q)}$: neighbor set surrounded by an error ellipse

  $s_j^{(q)}$: $n_j^{(q)}$ - $c_j^{(q)}$

  For j = 1: K

  for all $x_s \in s_j^{(q)}$ and in order of distance from centroid $\mu_j^{(q)}$

  if $J\left(\ldots, c_j^{(q)}, \ldots\right) < J(\ldots, c_j^{(q)} \cup x_s, \ldots)$,

  then $c_j^{(q)} = c_j^{(q)} \cup \{x_s\}$.

  end

  ③ Repeat until the object function J does not change.

III. Numerical Evaluations

In this section, we verify the derived survival conditions and validate the proposed node allocation method by performing a numerical analysis. Five robots are targeted, and their parameters are listed in Table II. The three sets of energy nodes are listed in Table III.

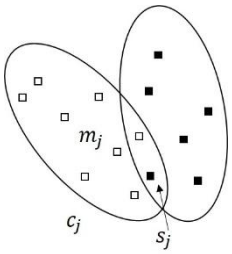

Figure 6. Covariance error ellipse of a cluster.

TABLE II. Robot Sets for Numerical Evaluation.

Robot Number	1	2	3	4	5
R (m/s)	0.2	0.1	0.15	0.3	0.25
P_{move} (W)	10.1	8.5	10.0	12.5	10.5
P_{work} (W)	8.0	4.0	12.3	7.5	7.1
P_{sleep} (W)	2.0	1.5	2.2	1.7	2.1
P_{rest} (W)	4.2	5.6	6.1	3.5	4.5
Sleep function	Yes	Yes	No	No	No

TABLE III. Node Sets for Numerical Evaluation.

Node set	1	2	3
Number of nodes	6	15	30
Installation area	500 ×500 m	500 ×500 m	1600 ×1600 m
Node Power Capacity	Varying	2–5 W, 52.5 W total	2–5 W 105 W total
Storage Capacity	Varying	9072 KJ	18114 KJ

First, the survival conditions given in (13) and (17) are numerically verified. In the numerical analysis, the parameters of Robot 1 in Table II were used. The survival area was obtained using the energy generation rate ε_{total} and the total travel distance d as variables. Fig. 7 illustrates the survival area of the robot with respect to ε_{total} and travel distance d when the total storage capacity is two days of energy production.

For the simulation, we placed six energy nodes randomly in a 500 × 500 m flat area, summarized as Node Set 1 in Table III with the power capacity condition of Points A, B, and C in Fig. 7. Points A, B, and C represent the survival region without sleep ability, survival region with sleep ability, and non-viable region, respectively. The mobile robot visits the nodes along a Hamiltonian path spanning a total distance of d = 1,469.8 m. Each energy node has a random energy generation rate, and total energy generation rate ε_{total} = 20, 10, and 2.5 W for Points A, B, and C, respectively. The power consumed for the tasks performed by the robot are uniformly distributed between 0 W and 16 W, with the average being 8 W, and the robot working times randomly range between 10 s and 60 s. If necessary, the sleep state is entered during operation by following the proposed recharge strategy.

Fig. 8 illustrates the amount of energy R(t) in the robot immediately after the recharge cycle. In Case A without sleep ability and Case B with sleep ability, the robot survived. By contrast, in Case C, even with the sleep ability, the robot starved, as predicted using (13) and (17). Under the conditions of Point B, a robot without any sleep function starved.

For testing the node allocation algorithm, Node Set 2, summarized in Table III, was placed in an area of 500 × 500 m. These nodes were assigned to Robots 1, 2, and 3, the parameters of which are listed in Table II. The weighted utility of the robots U_w was defined and used as the object function *J*. Let u_i be the utility of robot *i*, as in (28). U_w was then defined as the weighted sum of u_is, as in (29), where w_i denotes weight and is the P_{work} of robot *i* in this simulation. Therefore, *J* represents the average work of the robots per unit time. The expected utility u_i at equilibrium can be computed using (14), (21), and (22).

$$u_i = \frac{t_{work\_i}}{t_{work\_i}+t_{sleep\_i}+t_{recharge\_i}} \tag{28}$$

$$J = U_w(c_1, \ldots, c_K) \triangleq \frac{\sum_i w_i u_i}{K} \tag{29}$$

Fig. 9 (a) illustrates the initial allocation result obtained using the k-means algorithm, and Fig. 9 (b) illustrates the node allocation result adjusted using the proposed node reallocation method with α = 3. In this procedure, the value of U_w increased from 2.89306 to 5.3240. However, the degree of improvement was affected by the positions of the initial centroids. The weighted utility values obtained using the allocation methods are listed in Table IV. The data in the last column of the table is a result for comparison, and it is the maximum weighted utility value that can be obtained when one node is assigned to each robot as a base node and the remaining nodes are assigned arbitrarily. As the number of nodes increases, it becomes increasingly difficult to determine the optimal value because of increasing computational burden. If the area and capacity of the energy nodes are equally allocated to the robot, the weighted utility is expected to be 2.97. Finally, Node Set 3 is assigned to the five robots summarized in Table II (Robots 1–5). Figs. 10 (a) and (b) illustrate the initial and adjusted allocation results, respectively. U_w increased from 3.9 to 5.3. Fig. 11 illustrates the amount of energy *R(t)* in the robot immediately after the recharge cycle. Fig. 12 illustrates the utility of each robot, where the dashed line is the expected utility.

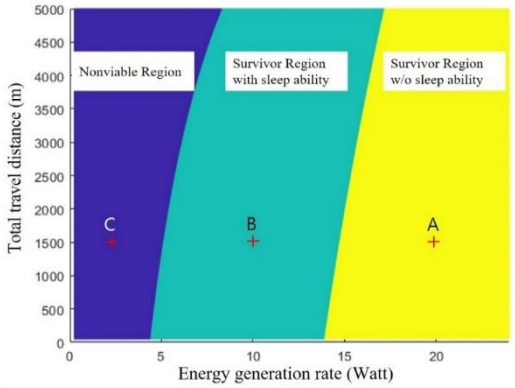

Figure 7. Robot survival region.

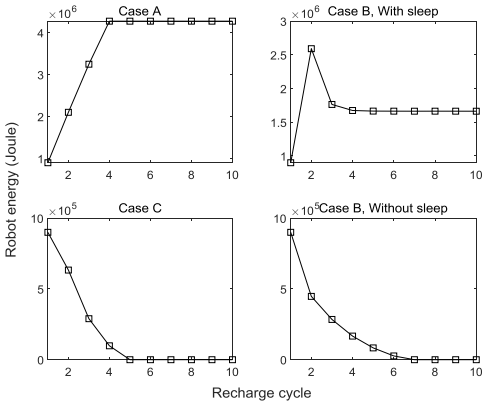

Figure 8. Energy stored in robot after recharge cycle.

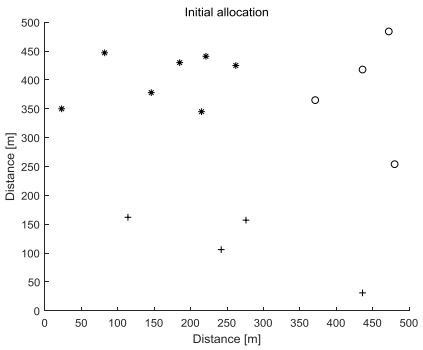

(a) Initial allocation

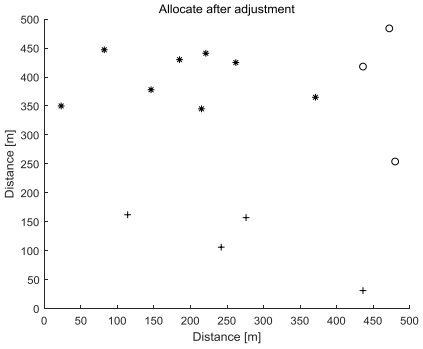

(b) After adjustment

Figure 9. Energy node allocation result for Node Set 2 (*: Robot 1, +: Robot 2, and o: Robot 3).

TABLE IV. WEIGHTED UTILITY VALUES COMPUTED USING DIFFERENT ALLOCATION METHODS.

	Classical k-means	Proposed Method	Optimal result
Weighted utility	2.89306	5.3240	5.4337

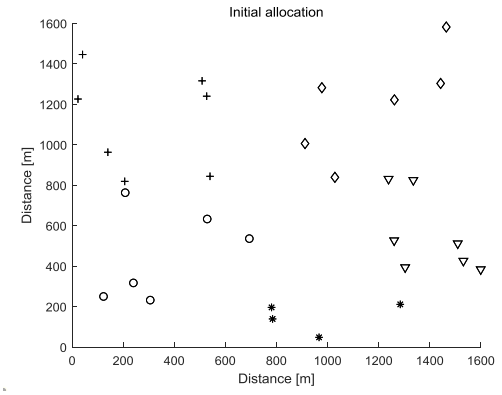

(a) Initial allocation

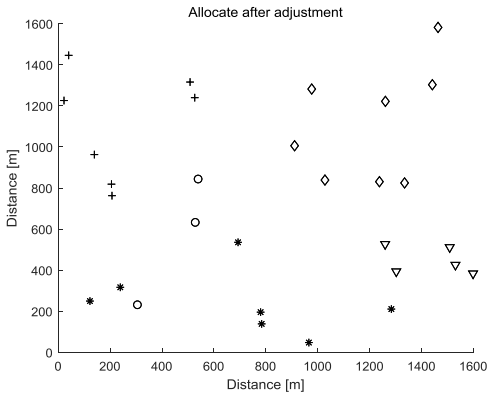

(b) After adjustment

Figure 10. Energy node allocation result for Node Set 3 (+: Robot 1, o: Robot 2, *: Robot 3, ∇: Robot 4, and ◊: Robot 5).

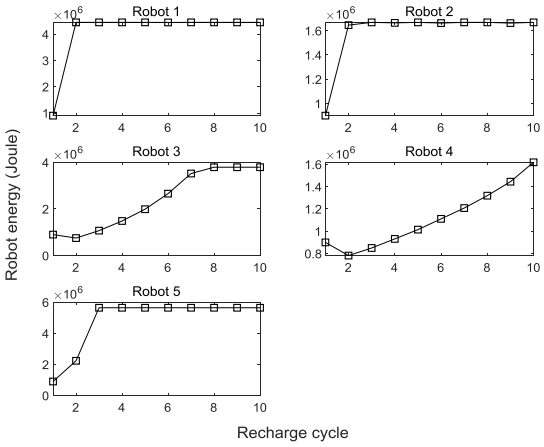

Figure 11. Energy stored in robot after recharge cycle in Node Set 3.

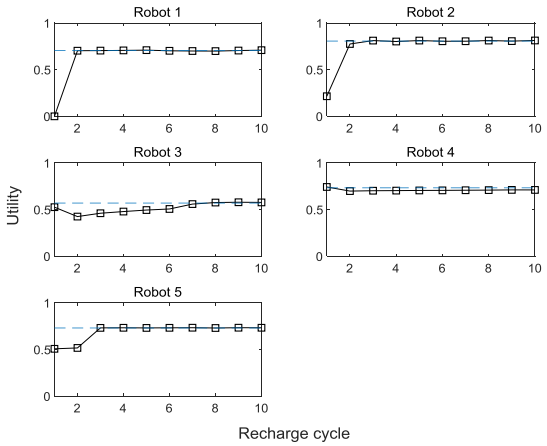

Figure 12. Utility of each robot in Node Set 3.

IV. EXPERIMENTS

A. Experimental Setup

An experiment was conducted to verify the feasibility of a multi-robot system that survives on small-scale renewable energy. However, only docking and charging experiments were conducted for one energy node. The long-term survival experiment of the multi-robot system could not be conducted in this study because the robot system was not adequately reliable yet. A considerable portion of the experimental setup was constructed in a previous study [8], and for the sake of completeness, the relevant content is presented again in this paper.

The experiments were conducted under a new experimental scenario. The experimental energy node comprised a thermoelectric energy module (TEM) to generate electricity by using waste heat [17], as illustrated in Fig. 13. By piling up TEMs, we built two TEM generators; the specifications of the first generator (Station 1) are listed in Table V. The capacity of the second generator (Station 2) was half that of the first generator. Table V summarizes the voltage, current, and power generated by the TEM used in this experiment. Given the converter, charger, and battery efficiency, the overall energy generation rate was estimated to be 4.6 W.

Turtlebot3 was used in the experiment. It was equipped with a laser scanner and a webcam for navigation and object recognition, respectively. Because this robot used a Raspberry pi 3 board as the controller, it did not have a sleep function; however, its power consumption was extremely low (1.4 W) in the idle state. The robot parameters derived from the experimental results are listed in Table VI, where P_{move} is the power consumed by the robot when traveling on flat terrain at 0.2 m/s, and P_{work} is set arbitrarily depending on the robot operation scenario.

From (17) and under these experimental conditions, it was predicted that the robot could survive with two energy nodes—Stations 1 and 2—if they are installed in an area of 20 × 20 m, and their total ES capacity is 198.7 KJ. $t_{work\_eq} = 0.8\,h$, $t_{sleep\_eq} = 3.4$ h, $t_{charge\_eq} = 3.8$ h, and u = 0.1 were expected. The process from when a robot

approaches an energy node until the time it is docked at the energy node is depicted in Fig. 14.

B. Docking Experiment Results

After the robot approached the energy node, it recognized the node by using image information and a single shot detector (SSD) algorithm [18]. Fig. 15 illustrates the recognition and identification results for the two types of energy nodes considered herein. The robot then estimated the position and direction of the energy node and the predetermined transmission coil pad. The transmitting and receiving coils must be aligned accurately to achieve a high transmission efficiency. Fig. 16 illustrates the final docking with the charging coil. A small artificial marker was used to calculate the robot's pose for precise alignment of the robot and the charging coil. Fig. 17 illustrates the robot's trajectory from several initial positions until it is docked at the charging coil.

Figure 13. Thermoelectric energy module.

TABLE V. THERMOELECTRIC ENERGY MODULE (TEM) OUTPUTS.

Voltage (V)	Current (A)	TEM power (W)	Estimated available power (W)
13.61	0.66	8.98	4.6

$\Delta T = 64℃$ ($T_H = 168℃$)

TABLE VI. ROBOT PARAMETERS.

P_{move}	P_{rest}	P_{sleep}	P_{work}	μ	η
10.1W	4.2 W	1.4W	8W	15W	0.5

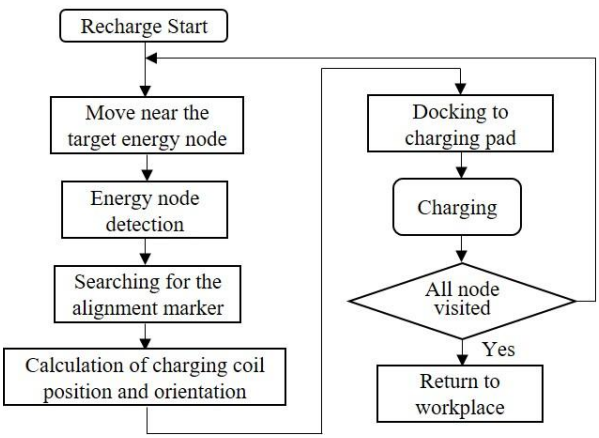

Figure 14. Robot charging process in the experiment.

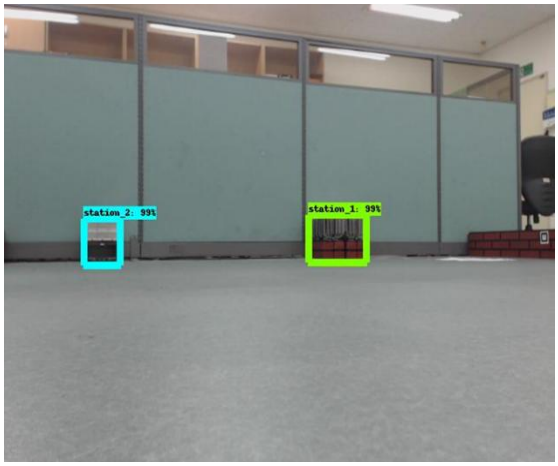

Figure 15. Energy node detection.

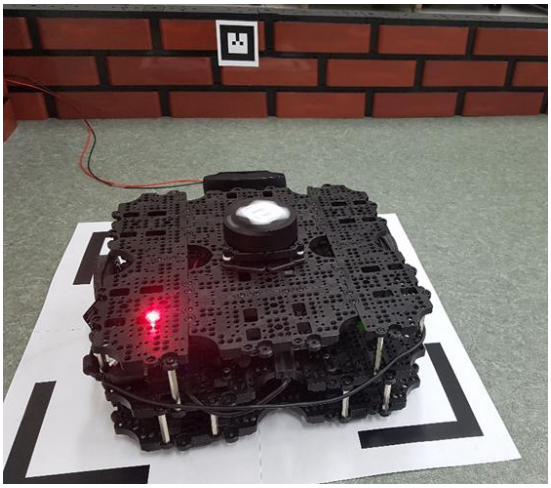

Figure 16. Docking with the charging coil.

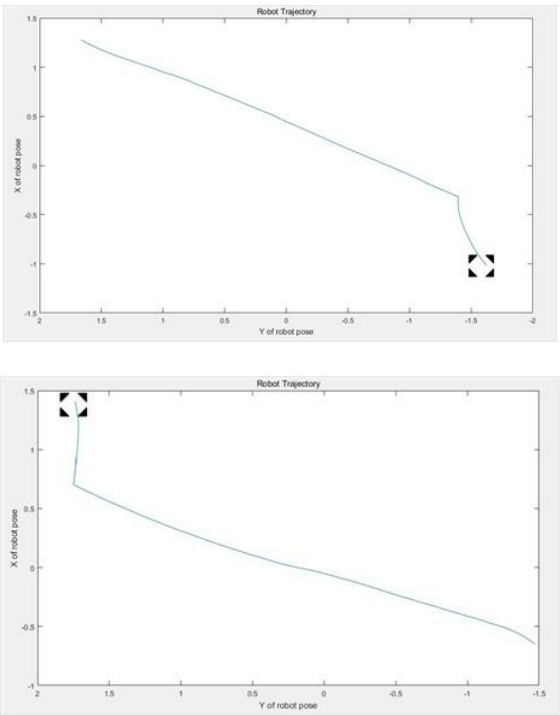

Figure 17. Robot trajectory until it is docked to the charging coil.

V. Conclusion

In this study, we proposed a robotic system in which multiple mobile robots are maintained in an operational state by using the energy generated by small-scale renewable energy sources distributed over a large area. The electrical energy produced by the small-scale generators was stored in a battery and then transferred to the robots through WPT. The survival conditions of the robot system were derived based on the energy production–consumption equilibrium condition, and a heuristic method for allocating energy nodes to each robot was proposed. Previous robot energy autonomy studies [5,6] considered only the method of supplying energy to the robots.

The primary contribution of this study is its investigation of whether a multi-robot system can be maintained in an operational state by using distributed small-scale renewable energy sources and proposition of an energy node allocation method. The proposed node allocation method consists of two steps. In the first step, the k-means algorithm is used to create clusters of nodes close to each other. In the second step, the nodes located at the boundaries of these clusters are reallocated to improve the object function, which is weighted utility in this study. The results of a numerical analysis and simulation verified that the weighted utility improved when the proposed allocation method was used. However, the degree of performance improvement varied depending on the location of the initial centroids, which is considered a characteristic of the k-means method. For the experiment, we implemented two types of energy nodes comprising TEMs to verify the feasibility of the proposed multi-robot energy autonomy scheme. The robot recognized the energy nodes by using the SSD algorithm, and an artificial marker was used to accurately align the robot and transmission coil. In an experiment, the robot was docked to the charging coil with sufficient positioning accuracy for achieving high transmission efficiency. The results of this experiment confirmed the feasibility of multi-robot energy autonomy scheme.

In this study, battery self-discharge and aging were not considered. Thus far, the transmission speed and efficiency of WPT are low, which lengthens the charging time excessively. For realizing practical implementations of robot autonomy, these issues must be addressed in advance. In future studies, we plan to expand our research on energy nodes to systems (such as solar power generation) that can generate electricity only during a certain period of the day.

Conflict of Interest

The authors declare no conflict of interest.

Author Contributions

J. Kim conducted the experiment; C. Moon derived the equations and wrote the paper; all authors had approved the final version.

References

[1] T. Ngo, H. Raposo, and H. Schioler, "Potentially distributable energy: towards energy autonomy in large population of mobile robots," in *Proc. the 2007 IEEE International Symposium on Computational Intelligence in Robotics and Automation*, 2007.

[2] H. Schioler and T. Ngo, "Trophallaxis in robotic swarms - beyond energy autonomy," in *Proc. the 10th International Conference on Control, Automation, Robotics and Vision*, 2008, pp. 1526–1533.

[3] U. Kartoun, H. Stern, Y. Edan, C. Feied, J. Handler, M. Smith, and M. Gillam, "Vision-based autonomous robot self-docking and recharging," in *Proc. the World Automation Congress*, 2006, pp. 1–8.

[4] K. Koo and K. Shin, "Apparatus for automatic charging of the autonomous mobile robot and method for automatic charging used the same," Korean Patent 1020080060535, 2008.

[5] M. Khonji, M. Alshehhi, C. Tseng, and C. Chau, "Autonomous inductive charging system for battery-operated electric drones," in *Proc. e-Energy '17 Proceedings of the Eighth International Conference on Future Energy Systems*, 2017. pp. 322–327.

[6] A. Ravankar, A. A. Ravankar, Y. Kobayashi, L. Jixin, T. Emaru, and Y. Hoshino, "An intelligent docking station manager for multiple mobile service robots," in *Proc. the 15th International Conference on Control, Automation and Systems*, 2015. pp. 71–78.

[7] B. Li, B. Moridian, A. Kamal, S. Patankar, and N. Mahmoudian, "Multi-robot mission planning with static energy replenishment," *Journal of Intelligent & Robotic Systems*, vol. 95, pp. 745–759, 2019.

[8] J. Kim and C. Moon, "A robot system maintained with small-scale distributed energy sources," *Energies*, vol. 12, no. 20, p. 3851, 2019.

[9] S. Steinerberger, "New bounds for the traveling salesman constant," *Advances in Applied Probability*, vol. 47, 2013.

[10] J. Kim, S. Rho, C. Moon, and H. Ahn, "Imaging processing based a wireless charging System with a Mobile Robot," *Computer Applications for Database, Education, and Ubiquitous Computing, Communications in Computer and Information Science*, vol. 352, pp. 298–301, 2012.

[11] I. Cortes and W. Kim, "Autonomous positioning of a mobile robot for wireless charging using computer vision and misalignment-sensing coils," in *Proc. the Annual American Control Conference*, 2018, pp. 4324–4329.

[12] A. Junaid, A. Konoiko, Y. Zweiri, M. Sahinkaya, and L. Seneviratne, "Autonomous wireless self-charging for multi-rotor unmanned aerial vehicles," *Energies*, vol. 10, 2017, p. 803.

[13] C. Rahn and C. Wang, *Battery Systems Engineering*, Wiley, 2013.

[14] Y. Mei, Y. Lu, Y. Hu, and C. Lee, "A case study of mobile robot's energy consumption and conservation techniques," in *Proc. 12th International Conference on Advanced Robotics*, 2005, pp. 492–497.

[15] R. Duda, P. Hart, and D. Stork, *Pattern Classification*, Wiley-Interscience, 2001.

[16] X. Wang, C. Xu, S. Duan, and J. Wan, "Error-ellipse-resampling-based particle filtering algorithm for target tracking," *IEEE Sensors Journal*, vol. 20, no. 10, pp. 5389–5397, 2020..

[17] L. Bell, "Cooling, heating, generating power, and recovering waste heat with thermoelectric systems," *Science*, vol. 321, no. 5895, pp. 1457–1461, 2008.

[18] R. Shanmugamani. *Deep Learning for Computer Vision*, Packt, 2018.

Jaehyun Kim is a master student at School of Electrical Engineering, Kookmin University, Seoul, Republic of Korea. He graduated from the bachelor's program at Kookmin University in August 2017.
His research interests are mobile robot navigation, wireless power transfer application for mobile robot and ROS programming.

Chanwoo Moon is a professor at School of Electrical Engineering, Kookmin University, Seoul, Republic of Korea. He graduated from Seoul National University with a Bachelor, Master and PhD degree of Electrical Engineering in 1989, 1991 and 2001, respectively.
His research interests are mobile robot navigation, motor control and vehicle electronics